Available online at www.sciencedirect.com
SCIENCE DIRECT®
Remote Sensing of Environment 87 (2003) 136–147
Remote Sensing of Environment
www.elsevier.com/locate/rse

Use of the Topex–Poseidon dual-frequency radar altimeter over land surfaces

Fabrice Papa*, Benoît Legrésy, Frédérique Rémy

Laboratoire d'Etudes en Géophysique et Océanographie Spatiales, Centre National d'Etudes Spatiales, 18, Avenue E. Belin, 31400 Toulouse, France

Received 27 January 2003; received in revised form 8 April 2003; accepted 17 April 2003

Abstract

The capability of NASA radar altimeter Topex for land surface studies at regional or global scale is investigated. The analyzed data, available since mid-1992 consist of dual-frequency backscattering coefficients values (Ku and C band) estimated at the nadir pointing angle along the satellite tracks between 66°S and 66°N and averaged in 0.75° ground resolution cell. Mean global backscatter images of the entire land surfaces are presented in Ku, C band and the difference C−Ku. Statistics and major temporal signals over nine entire years are also presented at a global scale. Finally, temporal profiles of backscatters are extracted for main land types (desert, tropical forest, wet and dry savanna, boreal regions, ice sheet) to validate the dataset and to analyze radar response to land surface variability through 9 years. Results indicate the high capabilities of Topex–Poseidon (T–P) radar altimeter data for monitoring snow-covered regions at global and regional scale. The use of dual-frequency measurements can also improve methods developed with single frequency radar altimeter over complex vegetated areas. The complementarities for future synergy with wind-scatterometer or satellite imagery data over continents look also promising because of the T–P 10-day repeat cycle, a 10-year span dataset and a future better spatial resolution with combination of other dual-frequency altimetry missions such as ENVISAT or Jason.

Keywords: Remote sensing; Radar altimeter; Topex–Poseidon; Continental surfaces

1. Introduction

Monitoring continental characteristics at global or regional scales are essential to better understand land surface processes and their interactions with the atmosphere. In this context, monitoring vegetation, ground wetness, snow, inland water or soil parameters has been operational for many years using different space-borne sensors operating in different part of the electromagnetic spectrum, such as those operating in visible or infrared domains (AVHRR (1981)) (Birkett, 2000; Moulin, Kergoat, Viovy, & Dedieu, 1997) or those operating in the microwave domain, such as the passive microwave radiometers (SMMR (1978), SSM/I (1987)) (Justice, Townshend, & Choudhury, 1989; Njoku & Li, 1999; Sippel, Hamilton, Melack, & Novo, 1998). The observation of continental surfaces with active microwave sensors started a few years ago with the launch of C-band (5 GHz) wind-scatterometer on board the European remote sensing satellites ERS-1 (1991) and ERS-2 (1995). Initially designed for the study of winds over oceanic surfaces (Johnson, 1980), the potentials of wind-scatterometers over continents were demonstrated for monitoring global vegetation or soil characteristics (Frison & Mougin, 1996a) and opened a new way to investigate continental surfaces using active microwave instruments on board satellites.

In the same context, satellite-altimeter radars, which are nadir-pointing active microwave sensors initially reserved for operating over the ocean and making accurate measurements of sea level (Fung & Cazenave, 2001), exhibited very early on strong capabilities in the study of continental surfaces (Zwally, Binschader, Brenner, Martin, & Thomas, 1983), with at this time, a main interest in the construction of a precise topography for ice-covered continents such as Antarctica or Greenland (Remy, Schaeffer, & Legresy, 1999). The excellent accuracy of the height measurements also enables the survey of the ice-sheets surface elevation, the estimation of their mass balance or their flow, and the recovery of pertinent geophysical parameters such as snow pack characteristics and surface roughness (Legresy & Remy, 1997).

* Corresponding author. Tel.: +33-5-61333006; fax: +33-5-61253205.
E-mail address: fabrice.papa@cnes.fr (F. Papa).

0034-4257/$ - see front matter © 2003 Elsevier Inc. All rights reserved.
doi:10.1016/S0034-4257(03)00136-6

In parallel, the ability of radar altimeters to monitor continental water surfaces and measure their stage elevation has been also demonstrated over a wide variety of inland water bodies (Birkett, 1995; Cazenave, Bonnefond, & DoMinh, 1997). However, because altimetry is a profiling and not an imaging technique, it is applicable mostly to large water bodies, with a main interest in the survey of lakes, large rivers or flood plains level fluctuations. This application has been further extended to study regional hydrological systems of areas in Africa or South America (Birkett, 2000; Mercier, Cazenave, & Maheu, 2002) or as a validation technique for water level changes measured with interferometric processing of synthetic aperture radar data of large Amazon lake (Alsdorf, Birkett, Dunne, Melack, & Hess, 2001).

Recently, by using the radar altimeter backscattering coefficient, that is proportional to the power returned at the instrument, Papa, Legresy, Monard, Josberger, and Remy (2002) and Papa, Mognard, Josberger, and Remy (2001) demonstrated new capabilities of satellite altimetry over continents to survey terrestrial snow covered regions. Papa et al. (2001) indeed showed over the Northern Great Plains of the USA that the presence of snow cover drastically decreased the value of the backscattering coefficient when compared to the backscatter value of the same free-snow area. This evolution of the backscatter allows determining the beginning and the end of the snow period and, thus the decrease in backscatter enables to estimate snow depth evolution (Papa et al., 2002), two of the snow parameters listed by Allison and Goodison (2001) that are essential for hydrological and climate change studies of the high latitudes.

At this time, global study using inland altimetry is poorly developed and only one image shows the global distribution over continents of mean values of vertical incidence radar altimeter backscatter with the single frequency Ku band Seasat altimeter measurements (Guzkowska et al., 1990). Apart for large regions of polar ice-sheets, the development of radar altimetry over land surfaces is so still limited to regional studies (Birkett, 2000) and by the only exploitation of the classical single Ku band frequency measurements.

The aim of this paper is to describe the potentials of radar altimeter backscattering coefficient measurements for monitoring spatial and temporal signatures of global land surfaces. For this purpose, we used data from the radar altimeter on board the CNES/NASA satellite Topex–Poseidon (1992) (T–P), which has a 9.91-day repeat cycle. Particularly, the main interest resides in the use of NASA Radar Altimeter (NRA) Topex that is the first dual-frequency active microwave sensor at nadir and provides measurements in Ku (13.6 GHz) and C (5.4 GHz) bands.

The backscattering coefficient results from two contributions: a surface scattering echo that is the scattering by an interface between two dissimilar media and a volume scattering echo that is the scattering by particles contained inside a medium. These two contributions depend on the land target characteristics, the radar footprint (depending on surface roughness) and the quantity of surface scatterers within the footprint. Three different simple cases can be encountered over land surfaces described as follows:

- The return signal is only due to the surface echo, controlled by the dielectric constant and the surface roughness of the target. Because Topex–Poseidon is a nadir-looking instrument, the surface echo is not negligible and can even be the dominant term. Over land, this situation is expected over inland water surface, inundated soils, melting snow, several solid bare soils...
- The return signal is due to reflecting surfaces located under volumetric scatterers. The averaged signal is due to the underlying surface echo attenuated by the extinction of the radar wave within the scattering medium. Over land, this situation is expected over sparse forests, over inundated forests, over dry snow-covered areas...
- The return signal is due to reflecting surfaces situated above volumetric scatters. The averaged signal is due to the surface echo and the volume echo that results from the underlying volume scattering. Over land, this situation is expected for dry or arid areas, wet snow-covered areas, and some vegetated areas...

The last two cases, where the averaged signal depends on the volume scattering and the extinction within the medium, are frequency dependant. With its dual-frequency, T–P radar altimeter will detect the difference in scattering and extinction in the medium; unless otherwise specified, we assume in this study that the relative difference in backscatter from dual-frequency is mainly due to the difference in the penetration of the waves in the target.

For the period from end-1992 to mid-2002, which represents a 10-year time-span dataset, dual-frequency NRA Topex backscattering coefficients measurements are processed and analyzed for the continental surfaces covered by the satellite tracks.

The satellite data are presented in Section 2. Section 3 presents the first results on a global scale and the geographical dynamics of backscatter over land surfaces. Section 4 deals with the seasonal and temporal behavior of the backscatter signal over nine consecutive years of Topex–Poseidon observations.

2. Datasets and methods

Topex–Poseidon was the first dual-frequency radar altimeter of a joint US and French mission initially developed to make accurate measurements of sea level (Zieger, Hancock, Hayne, & Purdy, 1991). From its launch in October 1992 to the present, the Topex–Poseidon 10-day repeat cycle, allows for the observations along its track of the whole oceans and continental surfaces from 66° latitude North to 66° latitude South. The NASA Radar Altimeter

Topex operates in Ku band (13.6 GHz frequency, 2.3-cm wavelength), and C-band (5.4 GHz frequency, 5.8-cm wavelength). The dual-frequency was initially designed to provide corrections on the height measurement errors due to the ionospheric delays on the signal. Even on continental targets, where variations in the surface elevation are important, measurements with both frequencies can be considered as simultaneous over a time interval of 0.1 s, corresponding to a 700-m along track distance (Remy, Legresy, Bleuzen, Vincent, & Minster, 1996). General characteristics and performances of the T–P NRA instrument can be found in (Rodriguez & Martin, 1994).

In this study, we only analyze the backscattering coefficients measurements from NRA Topex in C and Ku band expressed in decibels (dB) that are extracted from the Aviso database (merged T–P Geophysical Data Records, GDRs, AVISO, 1996).

T–P equatorial ground track spacing is about 300 km and its swath width only amounts of few kilometers. For each 10-day T–P cycle (the satellite pass over the same point every 9.91 days), the backscatter measurements in each frequency along the satellite tracks are averaged every 0.75° in latitude and longitude and weighted with respect to the exponential of the square distance with a decorrelation distance of 150 km. This choice is indeed a good compromise between the enhancement of the spatial resolution and the diminution of the noise of the data. At 1-s scale (7 km along the satellite track), the backscattering coefficient precision is less than 1 dB. At the equator, the mean number of values per 0.75° cell is 9 and 18 at 60° of latitude. So that the averaged precision at the scale of the 0.75° cell can be estimated around 0.33 dB at the equator and 0.24 dB at highest latitudes. To avoid contamination of land surface data with ocean measurements, especially for locations close to the coasts, we masked the data over the oceans.

For this study, 357 cycles of T–P satellite were available, that corresponds to a period from October 1992 to June 2002. However, only 332 cycles of T–P are computed for the calculation of statistical tools, such as the mean value, the standard deviation, the mean seasonal signals and the trend. Indeed, these 332 cycles of T–P data represents exactly 9 years of data, from 1st January 1993 to 1st January 2002 and prevent us from biases due to inhomogeneous time sampling and errors due to bad data from the first cycles.

3. First results on global scale

3.1. Mean and standard deviation global images analysis

Fig. 1 shows the mean value and the associated standard deviation of the T–P backscattering coefficients in Ku (a, b) and C (c, d) bands and the difference of backscattering coefficients C–Ku (e, f) over the land surfaces. The mean values and the standard deviations are calculated over 332 cycles as indicated in Section 2.

At a global scale, the backscatter values range from 0 to more than 25 dB for Ku band, that also means a factor of more than 300 for the power in term of logarithmic scale (the upper limit is 44 dB set by the T–P hardware constraint) and from a few dB to more than 30 dB in C band, giving an overall spatial dynamic higher than 25 dB.

For both bands, the backscattering coefficient is low over mountainous regions (< 7 dB in Ku band, < 12 in C band), which is directly due to the presence of topographic slopes, as the antenna pattern (aperture of the antenna is 0.6° in Ku band and 2° in C band) convoluted with the angle of incidence decreases the return power of the altimetric echo. This is particularly the case for typical mountainous regions such as the Himalayan, the Andes or the Rocky Mountains in the USA.

For both bands, high values of the backscatter are typical of very flat surfaces such as some parts of desert regions or large river basins, because of the specular return radar echo. For some areas of the Sahara, the mean value of the backscatter in Ku band is more than 15 dB and more than 20 dB in C band. The same comment applies to the Australian and Central Asian deserts. Large river basins have typical values of more than 23 dB in Ku band and 28 dB in C band. Since the presence of even small (~ 100 m) areas of free-standing water in the altimeter footprint can dominate the return echo, masking the signal from the corresponding land surfaces, it is not surprising that there exists a general correlation with bright echoes in both bands and well-known water areas, as shown by Guzkowska et al., (1990). This is the case for the Ob river basin in Russia (frozen during the winter) and the Ganges River in India.

The dominant and stronger signal of the standard deviation (STD) for both bands (higher than 4 or 5 dB) is located at latitudes up to 55° latitude north. This greatest variability is due to the seasonal presence of snow on these high latitudes that drastically decreases the backscattering coefficient values (Papa et al., 2002). Note the specific values of the STD around 3 or 4 dB in Africa or South America in the savanna areas, due to change in ground and vegetation characteristics during the rainy season. The regions with the smallest STD values (< 1 dB) are the mountains and some homogeneous parts of the deserts (Sahara, Takla Makan and Gobi close to China) or tropical forests (African rain forests or Amazonian rain forest).

Fig. 1c shows the results from the difference in backscatters C–Ku. The first remark in accordance with theory and previous observations is that this difference is always positive. For typical ocean surface, the mean value of the difference is about 4 dB (Chapron, Katsaros, Elfouhaily, & Vandemark, 1995). Over land, the difference of the backscatters C–Ku ranges from a few decibels to more than 11 dB, with a mean value for the whole continental surfaces close to 6.2 dB. Fig. 1e shows a typical spectral signature of the continental surface. High values of the difference C–Ku (>8 dB) are found in arid and desert regions: Sahara, Takla Makan (China), Gobi desert and Central Asia deserts. Lower

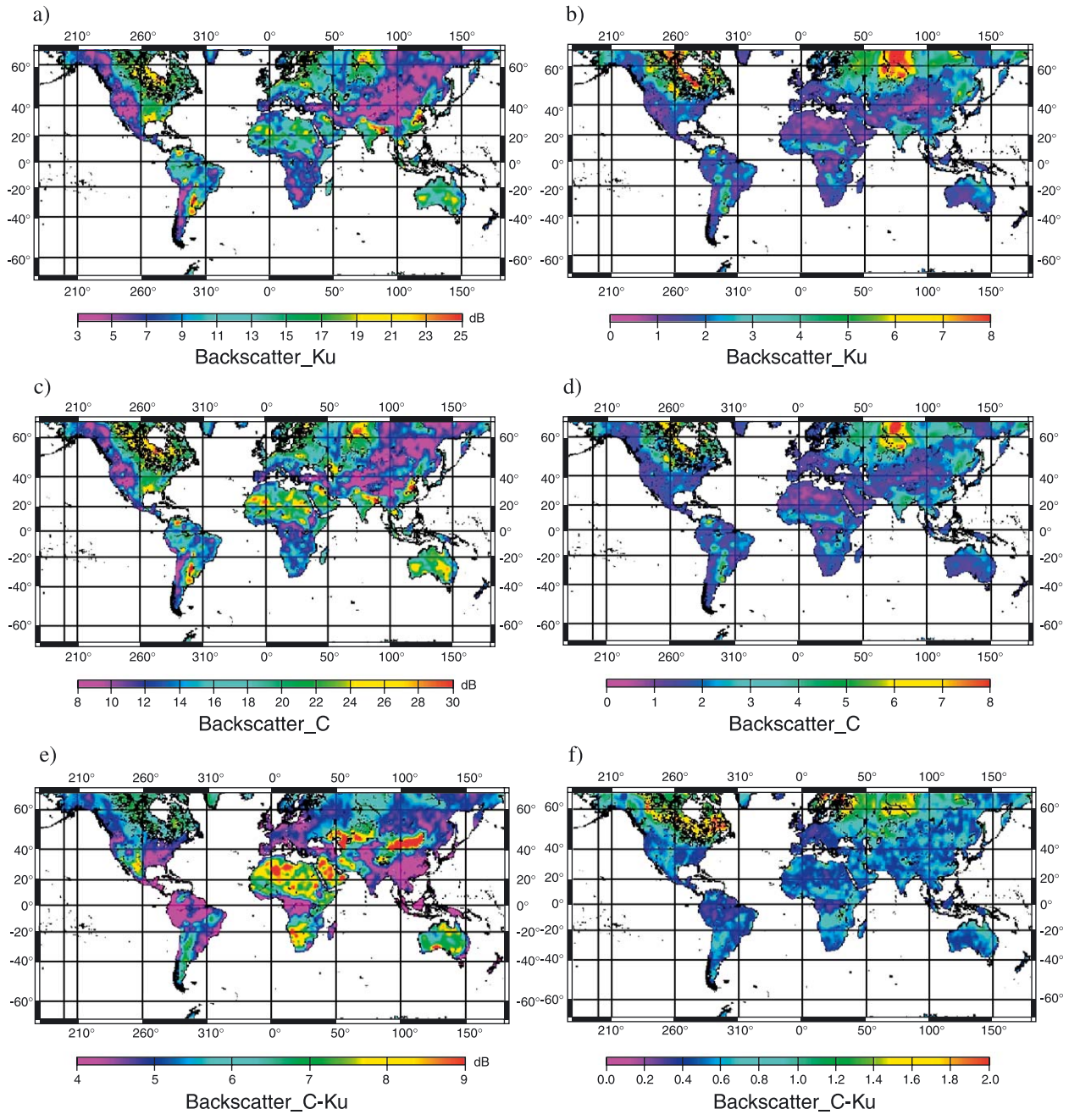

Fig. 1. Global variability of T–P radar altimeter backscatter coefficient from January 1993 to January 2002. (a) Mean value of the backscatter in Ku (dB). (b) Standard deviation of the backscatter in Ku (dB). (c) Mean value of the backscatter in C (dB). (d) Standard deviation of the backscatter in Ku (dB). (e) Mean value of the difference in backscatter C–Ku (dB). (f) Standard deviation of the difference in backscatter C–Ku (dB).

values of the difference C–Ku (< 5 dB) correspond to dense tropical rain forests of Africa, South America and South East Asia and forest of temperate regions. These regions are characterized by the smallest STD values (< 1.2 dB).

For the boreal forest, the mean value is higher (5 and 7 dB) than for other forests, because these regions are subject to seasonal snow cover and they have the highest values of the STD (>1.5 dB).

In conclusion, many types of surfaces can be clearly distinguished using C and Ku bands backscatters and C–Ku: tropical forests, inundated/non-inundated forests, grassland/open woodland, deserts, snow/ice-covered region and high mountains. The most striking feature is the close correspondence between these backscatter images and global vegetation map, for instance the Olson classification (1992) or classical surface elevation maps. Many spatial similarities can also be found with the synthesized world global images of backscattering coefficient provided by the 35-day repeat cycle of the C-band wind-scatterometer on board ERS satellite (Frison & Mougin, 1996b).

4. Seasonal anomalies and temporal signatures. Trends for 9 years

4.1. Seasonal signals at a global scale

The seasonal signals were computed using 332 cycles of T−P, from 1st January 1993 to 1st January 2002 and are namely referenced to the seasons of Northern Hemisphere. The mean winter signal is the difference between the mean value of all the cycles during the winter period of the Northern Hemisphere (we chose data of T−P cycles from December, January and February for every year from 1993 to 2002) minus the mean value calculated over the same 332 cycles of T−P. We processed the different seasons in the same manner as the winter season, selecting the March, April and May data for spring (not shown), June, July and August for summer, and September, October and November for autumn (not shown).

To introduce seasonal signals at the global scale for backscatter in Ku and C−Ku, a North−South latitudinal transect of the African continent was primarily chosen to show spatial and temporal variations along a surface gradient from desert to forests. The transect starts at latitude 28°N to 28°S at longitude 20°E. Results are shown in Fig. 2 for the averaged winter period (December, January, February for the 332 cycles of T−P) and the summer period (June, July, August). As expected, deserts and areas of dense tropical forest present a very stable Ku and C−Ku backscattering coefficients throughout the year. On the contrary, the north and south Savanna areas exhibits typical temporal signatures which can be related to the vegetation cycle and rainy seasonal cycle that modifies soil wetness (thus inverted when looking at the north and south parts of the transect).

At the global scale, the winter and summer signals shown in Fig. 3 for the backscatter in Ku (a, c) and C−Ku (b, d) show a strong zonal dynamic and exhibit such same behaviors for surfaces types closed to the ones encountered over the transect. This is particularly the case for regions ranging from 20°N to 20°S in latitudes for the Amazonian and Southeast Asian regions (dense tropical forests, savanna, inundated monsoon forest) and desertic areas, with a symmetrical opposite signal from the equator.

However, the greatest variability for Ku is for the latitude up to 55°N, with winter anomaly values for the boreal regions that reaches more than −4 dB. This signal corresponds to the presence of snow and will be further explained in detail in Section 4.2.1. For C−Ku, the winter anomaly has globally positive values over 1 dB attributed to the difference of penetration between both bands, since the snow cover attenuation is less for C than for Ku band.

4.2. Temporal signatures of backscatters for selected sites. Discussion of results

The temporal variations of T−P backscatters are now examined for selected sites with various surfaces types. The

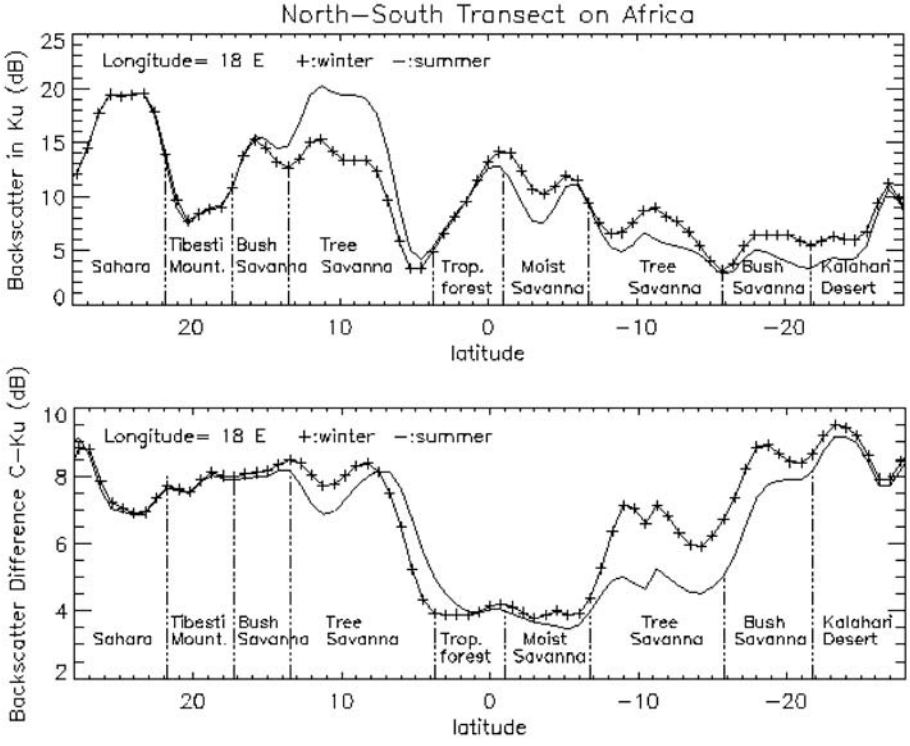

Fig. 2. Latitudinal transect over the African continent from 28 North to 28 South at longitude 20 East. Top: Mean values of the backscatter in Ku band (dB), for boreal winter period (+, December, January, February) and boreal summer period (June, July, August). Bottom: Mean values in C−Ku band (dB), for the boreal winter period (+, December, January, February) and boreal summer period (June, July, August).

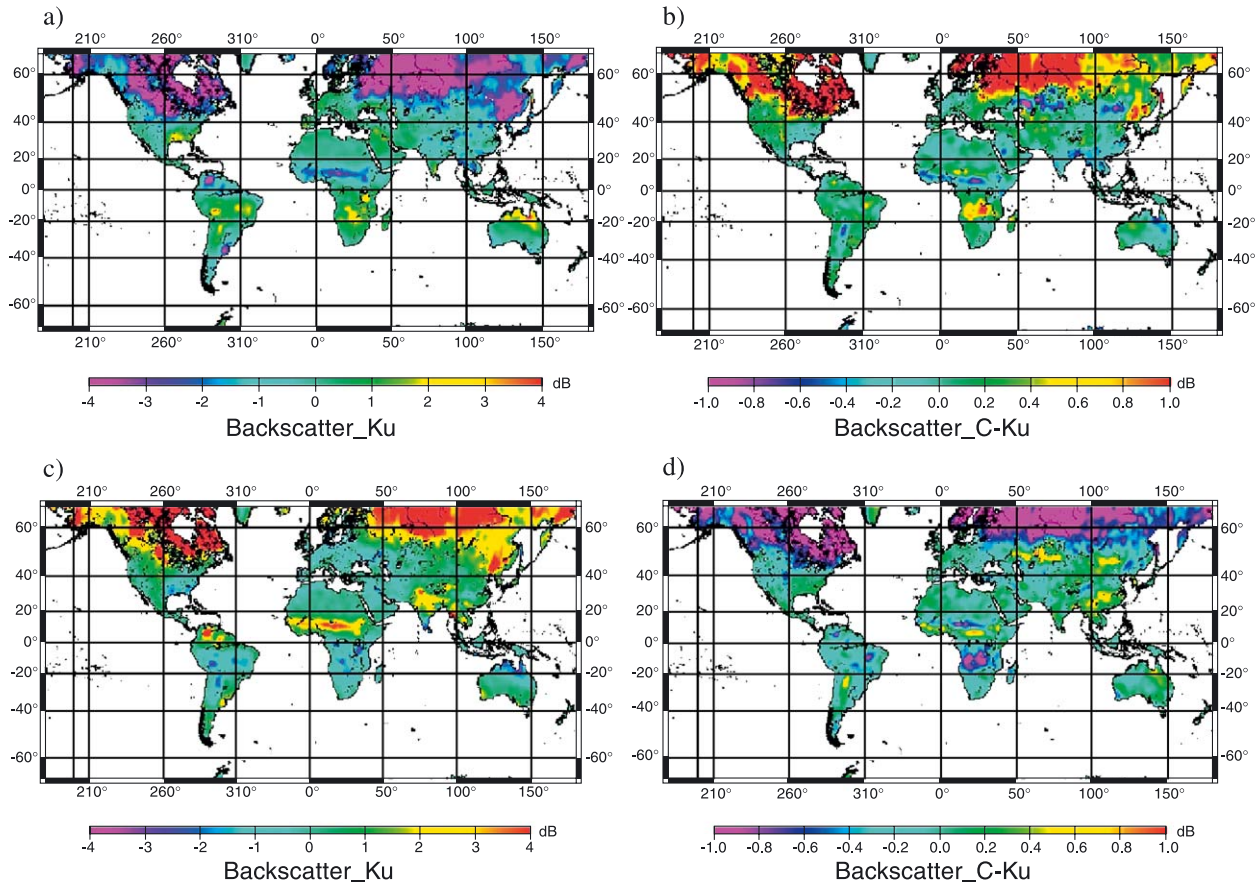

Fig. 3. Global scale maps of seasonal signal. (a) Mean boreal winter signal for the period December, January, February of the 332 cycles for the backscatter in Ku (dB). (b) Mean boreal winter signal for the period December, January, February of the 332 cycles for C−Ku (dB). (c) Mean boreal summer signal for the period June, July, August of the 332 cycles for the backscatter in Ku (dB). (d) Mean boreal summer signal for the period June, July, August of the 332 cycles for C−Ku (dB).

period considered is from October 1992 to June 2002 and enables to analyze the behavior of both signals for more than 9 years. Seven different sites were chosen to show the temporal evolutions of the backscatter in Ku band and C−Ku and illustrate different continental surfaces such as tropical forest, monsoon forest, savannas, deserts, boreal regions and ice sheets. The name of the selected sites, the surface types and the main statistics of the different temporal series are listed in Table 1. The general location of the sites is shown on the map (Fig. 4a) with a star and the associated letter referenced to the next figures. Results of the temporal profiles obtained for the backscattering coefficient in Ku band and for C−Ku are shown in Fig. 4 and the discussion is separated in three sections.

4.2.1. Temporal profiles for two sites. Validation of the T−P dataset with previous observations

Two sites over different land surfaces are selected including tropical forest (Fig. 4b) and deserts (Fig. 4c). These two sites represent land characteristics where the backscatter signal is well known from theoretical studies and corroborate previous observations with the single frequency Ku

Table 1
Surface characteristics and locations of the selected sites

Selected sites	Surfaces types	General location in Fig. 4a	Mean in Ku band (dB)	STD in Ku band (dB)	Mean in C−Ku (dB)	STD in C−Ku (dB)
Congo, Africa	Tropical forest	b	12.28	0.74	3.47	0.24
Takla Makan	Desert	c	5.79	0.59	7.30	0.41
Saharo−Sahelian band	Savanna	d	8.81	2.99	6.94	0.79
Amazon	Wet Savanna	e	9.18	1.46	5.07	0.67
East India	Seasonal forest	f	18.59	3.75	4.24	0.71
Ob Region, Russia	Boreal Regions	g	17.12	7.22	6.15	1.53
Greenland	Ice sheet	h	6.85	0.98	7.32	0.65

Mean and standard deviation of temporal profiles through 357 T−P cycles.

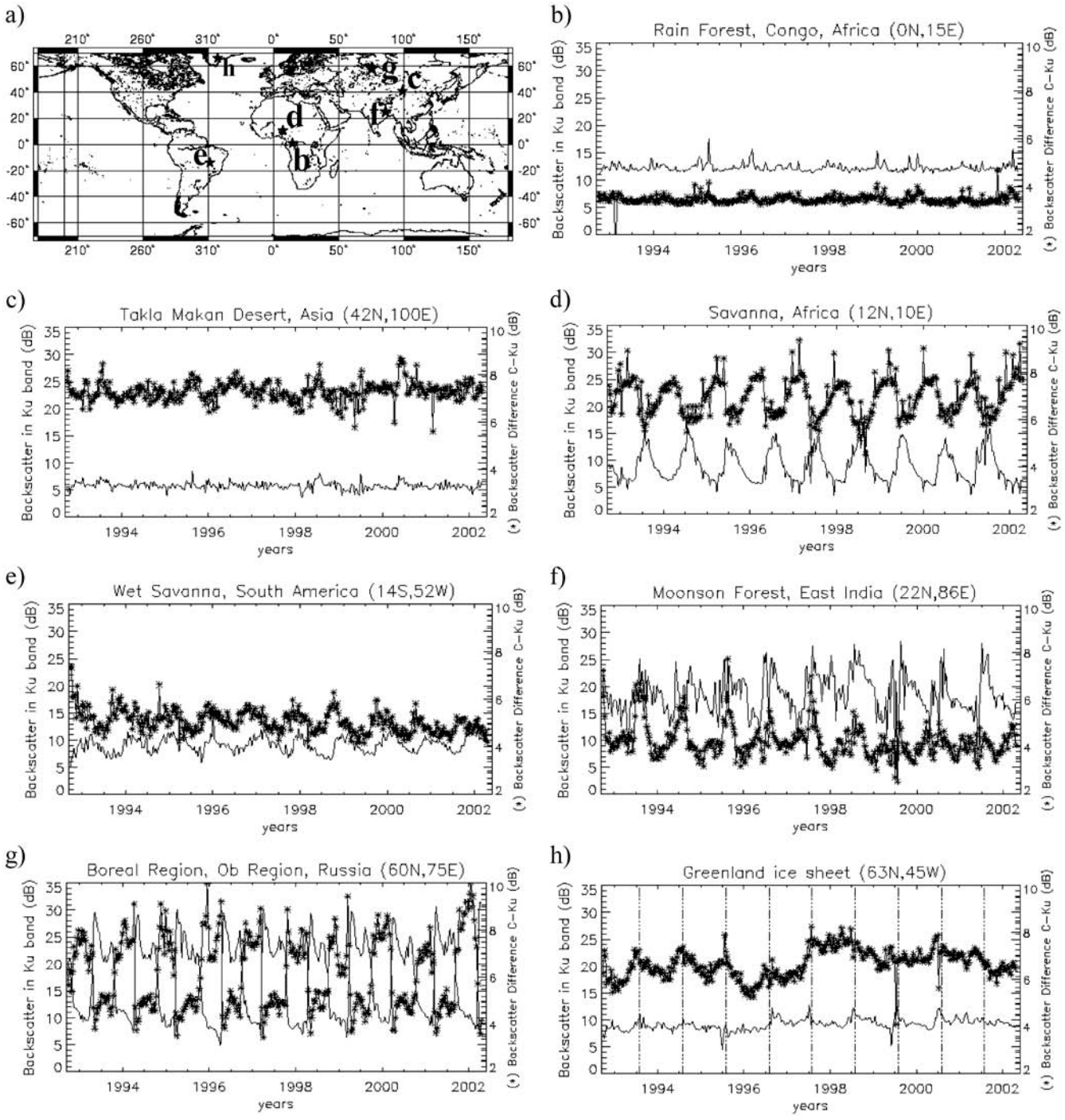

Fig. 4. Temporal profiles of seven selected sites from October 1992 to June 2002 for the backscatter in Ku (−) and C−Ku (*) in dB.

band altimeter on board Seasat or ERS satellites. This provides a validation of the T−P dataset.

• The African tropical forest exhibits a stable backscattering signal in Ku band over the 357 cycles, with values about 12 dB and a stable C−Ku signal with values around 3.5 dB. The signal in Ku is produced by the surface echo on the top of the forest canopy, dominated by leaves of large size (Ulaby, Moore, & Fung, 1986, pp. 1882–1992), and there is no penetration of the waves within the dense trees (C−Ku low). Small peaks around 1.5 dB for Ku are observed some years during the winter. This can be related to period of rain that modifies the dielectric constant by increasing the humidity content of the canopy. In the same time, C−Ku also increases by about 1 dB, as C band is more sensitive to wetness.

• The variability of the backscatter in Ku band from ERS1/2 altimeter over the Takla Makan region was found minimum in a previous study devoted to the calibration of

the radar altimeter RA-2 onboard the Environment satellite of the European Space Agency Envisat (Berry, Pinnock, & Wilson, 2000). There, the backscatter in Ku from T–P has low values around 5 dB and C–Ku shows high typical values of desert of about 8 dB, due to a difference of penetration between C and K in arid soils or sand dunes (Ulaby, Moore, & Fung, 1982, pp. 851–852). As expected for this extremely arid region, backscatters from T–P data exhibit a low variability over time, which is in agreement with Berry et al. (2000) and confirm the stable properties of this natural target over time that can be used at different frequencies for the calibration of future active microwave instruments. The C–Ku variations are also low (1 dB) and related to changes in penetration in the soil.

4.2.2. Temporal profiles for three seasonal vegetated sites

Three other sites over vegetated areas with a strong seasonal rainy cycle are selected. This includes Sahelian savanna located in Africa (Fig. 4d) and savanna located in South America (Fig. 4e), whose main characteristic difference resides in the underlying ground; over the Asian continent, one selected site is located in East India and consists of forest seasonally controlled by the monsoons (Fig. 4f). A number of data sets are potentially available to monitor such areas, but temporal/spatial resolution, cloud penetration and the ability of sensors to uniquely identified water or land or vegetation contribution to the signal are important considerations. Synthetic aperture radar can operate under both day/night and cloudy conditions, but wind and vegetation effects can cause complicated response from the surfaces of interest. NOAA/AVHRR satellites data offer images at multi-frequency channels twice a day over the same area, but cloud contamination particularly during the local wet season strongly affect the images. Seasonality of ERS windscatterometer backscattering coefficient over vegetated regions has been analyzed in Frison & Mougin, 1996b, but the signal, because of the 45° slide looking angle of the instrument and 35-day repeat orbit, provides only information on vegetation canopy and none on underlying surfaces.

Over areas such as wetland or inundated forest of Amazon basin or Chad basin, seasonality of altimeter backscattering coefficient has been previously studied by Birkett, (2000) and its values was used as a first-order filter to identify the presence of surface water. However, it was done using the T–P single Ku band measurements and within the backscatter 5–20-dB ranges. No clear divisions to identify the specific contributions from water, land and vegetation were identified. This first-order filter can be improved using the dual-frequency measurements.

- The temporal profiles of Ku and C–Ku for the area covered by the Sahelian savanna (Fig. 4d) are both marked by a strong seasonal signal that is strongly correlated with the seasonal evolution of the vegetation associated to the rainy season. During the dry winter season, the backscatter in Ku represents the return echo of the soil mixed with tree branches without leaves and the difference in backscatter C–Ku is mainly due to the difference of penetration in the soils and roughness sensitivity with values close to the ones encountered in the desert (8 dB). When the growth of vegetation starts, the backscatter in Ku increases from 7 dB to reach its maximum values around 16 dB during the period of maximum biomass in August. The signal in Ku band in summertime is controlled by the echo from the top of the trees (Ulaby et al., 1982, pp. 863–867). The evolution of C–Ku is in opposite phase with the Ku band behavior with a minimum value in August (6 dB). The C band signal must be partly controlled by the echo from the top of trees and the volume scattering of the canopy, which causes the C signal to increase. Since C band is less sensitive to the presence of leaves and can penetrate the foliage, the signal is also controlled by the underlying lower backscatter level ground echo, which is damped by the presence of vegetation (Ulaby et al., 1986, pp. 1869–1870).
- For South America, the selected wet savanna site (Fig. 4e) is vegetated, has a seasonal forest, but with a year round wet ground, which represents the main difference with previous site in Africa. For the 357 cycles, the backscattering in Ku exhibits a sinusoidal pattern due to a contrasted seasonal cycle, its maximum values around 12 dB being in January–February and minimum values around 8 dB at the end of July. The difference between July and January for C–Ku is about 1 dB. The yearly amplitude and phase of both signals differ when compared to the signal of the previous site of African savanna, because of the presence of leaves on the trees during the whole year. The temporal evolution of Ku and C–Ku shows a time lag that is due to a difference in the penetration depth in the medium (Sherjal &Fily, 1994). At the first stage of the growing season, the Ku band is sensitive to small new leaves, which amplify the return echo of the canopy, whereas the C band misses the first stage of the growth and its signal is still controlled by the echo from the underlying wet soil. When leaves are larger, C band increases, but less than Ku, as for the African savanna.
- The backscatters exhibit strong seasonal variations over the northeastern Indian forest (Fig. 4f), whose cycle is controlled by the monsoon regime. This scenario is equivalent to the scenario encountered over the two other forest sites. However, from May to July, the backscatter in Ku band drastically increases and C–Ku decreases to reach typical values of backscatters for flat-water surfaces (20 dB in Ku band, 3 dB for C–Ku). In that case, the backscatter behavior can only be attributed to the presence of flooded land.

4.2.3. Temporal profiles over two snow-covered selected sites

For the study of backscatters over snow-covered areas, one site retained is located in the boreal regions closed to the Ob river basin in the northern part of Russia (Fig. 4g) and one site over the Greenland ice sheet (Fig. 4h).

- The temporal evolution of backscatter in Ku and C bands for the boreal regions, mainly dominated by the seasonal cycle of snow, is particularly well understood

and described in previous studies devoted to the estimations of snow depths over the Northern Great Plains of USA (Papa et al., 2002, 2001).

There, the signal in Ku is marked by a strong seasonal cycle, with high values during the summer period (more than 20 dB) and low values for the winter (around 10 dB). The signal C−Ku is in opposite phase with Ku, with values around 5 dB for the summer period and more than 8 dB during the winter. A more precise description shows a notable peak for the backscatter in Ku (around 30 dB) and lower values for the difference C−Ku (4 dB) at the beginning of the springtime that are attributed to the presence of melted snow or flood. In the October−November period, the backscatter in Ku band starts to decrease in response to snow cover. The Ku signal over snow is the echo of the underlying ground surface, attenuated by the extinction of the wave within the snow cover. During the winter period, the backscatter evolution is thus related to snow depth evolution and snow pack characteristics. The backscatter difference C−Ku increases during the winter, as the C band is less attenuated than the Ku band by the snow (Papa et al., 2002). Using a simple model for dual-frequency backscatter, it is possible to retrieve snow depth evolution for the entire snow period. The drastic change in backscatters between winter and summer period also enables to determine the beginning and the end of the presence of the snow giving the duration of the snow period. Such information is not well recovered using slide looking angle passive microwave radiometer such as SSM/I, which cannot detect thin dry snow cover under 7 cm (Konig, Winther, & Isaksson, 2001). The 10-year T−P data will provide such information over the last decade and can be used in synergy with daily coverage passive microwave radiometer data long-time series.

• Over the Greenland ice sheet, the altimetric data have been studied in detail (Remy et al., 1996; Remy et al., 2001), but the usual aspect of such studies concerns the surface height evolution. However, it has been shown (Remy et al., 2001) that surveying the ice thickness over ice caps needs also to understand the altimeters echoes in detail to avoid misinterpretation. The Greenland surface here is mainly lying above 2000 m height and is year-round covered by a very thick snow pack (around 100 m from dry surface snow to pure deep ice). Thus, the amplitude of variations in Ku band is not very large (+ or − 1 to 2 dB). The microwaves penetrate in the dry snow and lead to a 6-dB average difference between C and Ku band backscatter with C band penetrating deeper. C−Ku varies seasonally in particular during the first 6 years of the profile. Vertical lines in Fig. 4h correspond to the 20th July of each year. The maximum of C−Ku occurs in summer during melt/refreezing and crust formation. In July 1997, a jump in (C−Ku) can be noticed (note also the peak in Ku) which must correspond to a hard crust formation or densification event. The signature of this crust or densification remains until 2001 with a progressive decrease, masking the seasonal variations. Dual-frequency altimetry in conjunction with other microwave sensors (radiometers/scatterometers) is very powerful tools to study the snow pack over ice caps (Remy et al., 2001).

4.3. Trends for 9 years

Trends that represent the overall increase or decrease of backscatter signal with time are calculated over the same 332 cycles of T−P data from 1st January 1993 to 1st January 2002, using a linear regression. They are shown in Fig. 5, for backscatter in Ku band (a) and C−Ku (b). Fig. 5c and d also shows the values of the correlation coefficient obtained when calculating the trend using the linear regression over the 332 cycles. Except for regions in black colors in Fig. 5c and d (correlation coefficient <0.1), the trend in Fig. 5a and b is significant at 95 % of confidence level. For example, the trend for Ku is not significant for most of the regions up to latitude 45 North, which is due to the strong seasonal signal over these areas. Note that removing the seasonal cycle with a sinusoidal behavior did not help to increase the level of confidence in these regions (not shown).

Fig. 5a shows large homogeneous areas with positive or negative significant trends; most of these areas exhibited high values of the backscatter (>15 dB) and significant values of the STD (>2 dB) when compared with Fig. 1a and b.

For the difference in backscatter C−Ku, Fig. 5b shows significant trends for the same homogeneous areas as for the Ku band, with however lower values and signs reversed. Note that for the northern-east part of Russia and for Alaska, the trend in Ku has a poor confidence level, whereas the trend is significant for C−Ku.

Three different regions have been chosen, where changes in surface characteristics over the last decade are well known and can be related to the observed backscatters trends: the Saharo−Sahelian band in Africa, the region of the Aral Sea in Kazakhstan, the boreal regions of eastern Russia and Alaska.

• For the Sahelian band in Africa, which corresponds to the limit between the Sahara desert and the Savanna forest, it is assumed in Section 4.2 that the seasonal signal of both backscatters is related to the vegetation cycle. Such observations of both backscatter trends could be interpreted as a decrease in vegetation density in these regions over the last decade. This is in agreement with studies on the desertification of West Africa related to climate changes (Fuller & Ottke, 2002) or the intensification of forest fires for the agriculture development (Gonzalez, 2001). . .

• The Aral Sea in Kazakhstan is in constant decrease since the 1970s (Micklin, 1988) which modifies regional climate and soils/vegetation characteristics around because of the presence of salt in the ground and the air (Kuzmina & Treshkin, 1997). It is impossible at this time to separate the different physical contributions, but for instance, the increase in Ku band and the decrease in C−Ku observed with the trends over the 9 years are in good accordance with the

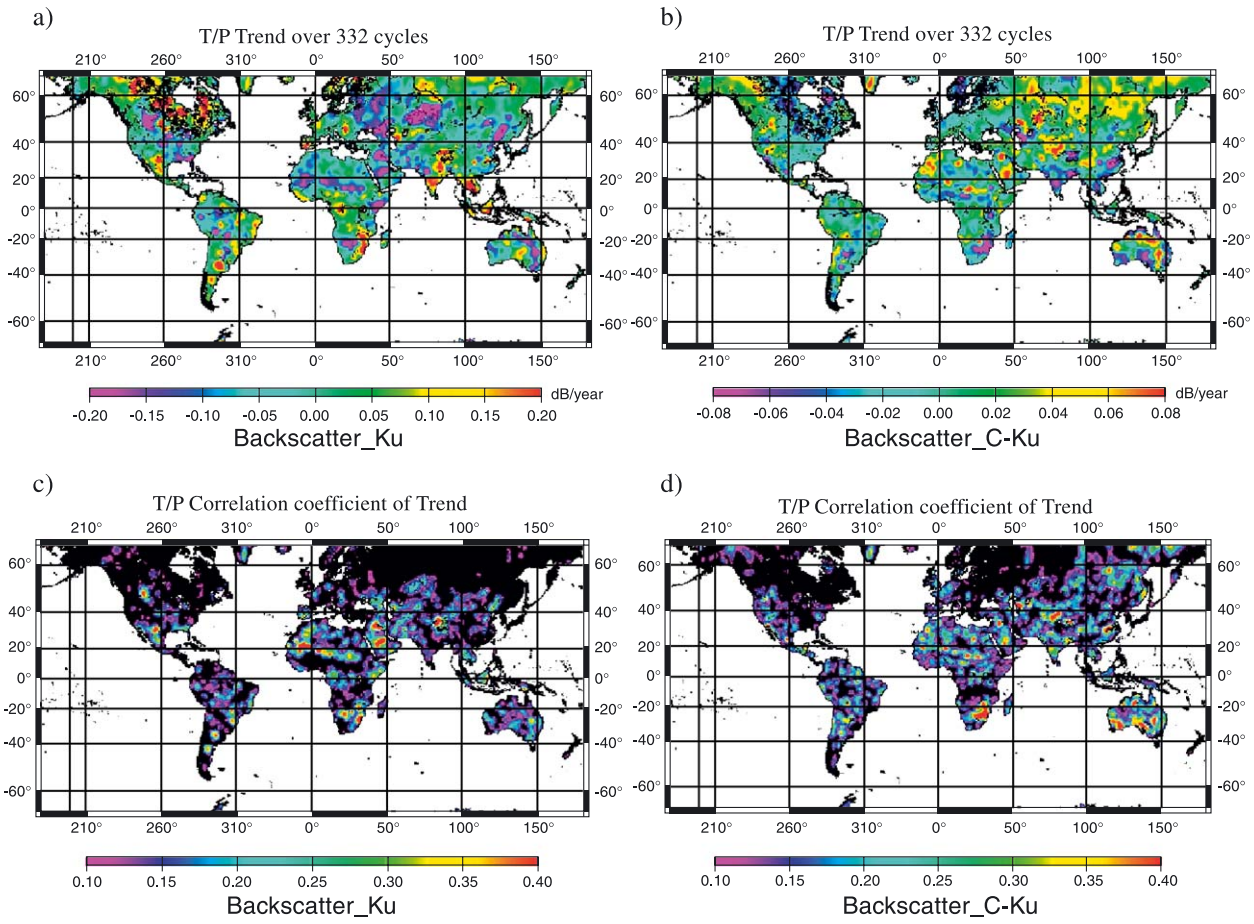

Fig. 5. Global scale maps of trends over 332 cycles. (a) Trends for Ku in dB per year. (b) Correlation coefficient of trend for Ku. (c) Trends for C−Ku in dB per year. (d) Correlation coefficient of trend for C−Ku.

decrease of snow depths and ice thickness and duration during the winter period (Kouraev et al., 2003) and the presence of salt in the ground that modifies the dielectric constant of soils.

• Snow pack thickness and extent, and the duration of the snow period are important parameters to characterize and understand climate changes. Global average surface temperature has increased by approximately 0.5 °C since the last half of the 19th century and climate models suggest that an anthropogenic global warming should manifest itself most strongly over the land in high latitudes. In that context, changes in snow cover characteristics take a special significance.

For the boreal regions of Eastern Russia and Alaska, the trend for Ku is not significant, as the seasonal variations of the backscatter in response to snow cover are too important (more than 15 dB) and at this time removing the seasonal cycle with a simple sinusoidal function did not help to increase the confidence level of the trend. However for C−Ku, the seasonal variations are smaller in values and the trend has a good confidence level. Over the last decade, the trend of C−Ku has a positive signal with a value more than 0.05 dB per year. Assuming that over snow, C−Ku is due to the difference of penetration between both waves in the snow cover, these observations suggest an increase of winter snow depth over the last 9 years, that is in accordance with the increase of snow depth over Eurasia and Alaska of 4% per decade (Allison & Goodison, 2001; Ye, Cho, & Gustafson, 1998).

In addition for snow-covered surface, note over the south Greenland a trend up to 0.08 dB per year is observed both in Ku and C−Ku. This must correspond to the densification event detailed in Section 4.2. It is noticeable that this trend occurs in both bands and is twice larger in C than in Ku, it corresponds well with the observation made in Papa et al. (2001) that the densification of the snow pack affects more the C band than Ku.

5. Conclusion and perspectives

The potential of the Topex NRA backscatters for land surface studies is investigated. Global maps of the world every 10 days (one complete cycle of T−P satellite) were processed in Ku, C band and the difference C−Ku for the entire period from October 1992 to June 2002. Mean global

map of the world land surface over 332 cycles in Ku, C and C–Ku with the associated standard deviation are obtained.

Data quality is assessed by evaluating backscatter response over well-known homogeneous and time-stable targets such as tropical forests and deserts. The expected behavior of the backscatters over these surfaces was excellent, with realistic values and stable evolution over the 9 years of data. Over snow-covered areas, results show that dual-frequency T–P data can be used for global studies of snow depth measurements or climate change of high latitudes. Radar altimeter will be useful in synergy with classical sensors for snow monitoring such as SSM/I radiometer. Over vegetated areas with a strong seasonal cycle, the dual-frequency measurements are promising to improve previous finding limited by the use of single Ku band T–P measurements. Clearly, more exploratory work with a modeled backscatter is required to recovery quantitative results on soil water content or vegetation properties. Future synergy with other space-borne sensors measurements such as passive microwave radiometer, active microwave wind-scatt and new imaging such as MODIS should also be considered.

In that context, the dual-frequency T–P radar altimeter data analysis shows the potentialities of this active microwave instrument at nadir pointing angle to monitor land surfaces at a global or regional scale. T–P data provides an excellent temporal resolution of $\sim$ 10 days. Major disadvantage is the poor spatial resolution of T–P radar altimeter, but the potential capacity to offer improved spatial resolution can be expected with the combination of other altimetric dual-frequency data such as ENVISAT (at S band, Ku band since March 2002) or Jason (at C and Ku bands, since December 2001).

Acknowledgements

This paper was written in the frame of the Observation des Surfaces Continentales par Altimetrie Radar (OSCAR) project. The data can be provided upon request to one of the authors. The authors thank the Centre de Topographie des Oceans (CTO) at the Laboratoire d'Etudes en Geophysique et Oceanographie Spatiale (LEGOS) for providing them the Topex–Poseidon radar altimeter data. We also thank Nelly Mognard from CESBIO-CNES for reviewing the English version of the paper and Monique Dechambre from CETP-Paris for her constructive comments. One of the authors, F.P. gets a grant from the Centre National d'Etudes Spatiales (CNES, France).

References

Allison, R. G. B., & Goodison, B. (2001). CLIC, Climate and Cryosphere Project. Science and Co-ordination plan. WRCP-114, WMO/TD.

Alsdorf, D., Birkett, C., Dunne, T., Melack, J., & Hess, L. (2001). Water level changes in large Amazon Lake measured with spaceborn radar interferometry and altimetry. *Geophysical Research Letter*, *28*(14), 2671–2674.

AVISO (1996). *AVISO User Handbook: Merged TOPEX–POSEIDON Products, AVI-NT-02-101-CN* (3rd ed.). Toulouse, France: CNES.

Berry, P. A. M., Pinnock, R. A., & Wilson, H. K. (2000). Land calibration and monitoring of ENVISAT RA-2 sigma0. *Proceedings of the ERS-ENVISAT Symposium, Gothenburg, Sweden*, CD-Rom SP-461.

Birkett, C. M. (1995). The contribution of Topex/Poseidon to the global monitoring of climatically sensitive lakes. *Journal of Geophysical Research*, *100*(C12), 25179–25204.

Birkett, C. M. (2000). Synergetic remote sensing of lake Chad: Variability of basin inundation. *Remote Sensing of Environment*, *72*(2), 218–236.

Cazenave, A., Bonnefond, P., & DoMinh, K. (1997). Caspian sea level from Topex/Poseidon altimetry: Level now falling. *Geophysical Research Letter*, *24*, 881–884.

Chapron, B., Katsaros, K., Elfouhaily, T., & Vandemark, D. (1995). A note on relationships between sea surface roughness and altimeter backscatter. *3rd International Symposium on Air–Water Gas Transfer* (pp. 869–878). Heidelberg, Germany: Heidelberg University.

Frison, P. L., & Mougin, E. (1996a). Use of the ERS-1 wind scatterometer data over land surfaces. *IEEE Transactions on Geoscience and Remote Sensing*, *34*(2), 550–560.

Frison, P. L., & Mougin, E. (1996b). Monitoring global vegetation in dynamics with the ERS-1 wind scatterometer data. *International Journal of Remote Sensing*, *17*(16), 3201–3218.

Fuller, D. O., & Ottke, C. (2002). Land cover, rainfall, and land surfaces albedo in West Africa. *Climate Change*, *54*, 181–204.

Fung, L. L., & Cazenave, A. (2001). *Satellite altimetry and earth science, A handbook of techniques and applications*. London, UK: Academic Press.

Gonzalez, P. (2001). Desertification and a shift of forest species in the West African Sahel. *Climate Research*, *17*(2), 217–228.

Guzkowska, M. A. J., Rapley, C. G., Redley, J. R., Cudlip, W., Birkett, C. M., & Scott, R. F. (1990). Development of Island Water and Land Caltimetry, ESA, CR-783/88/F/FL.

Johnson, J. W. (1980). Seasat—a scatterometer instrument evaluation. *IEEE Oceanic Engineering*, *OE-5*, 138–144.

Justice, C. O., Townshend, J. R. G., & Choudhury, B. J. (1989). Comparison of AVHRR an SMMR data for monitoring vegetation phenology on a continent scale. *International Journal of Remote Sensing*, *10*(10), 1607–1632.

Konig, M., Winther, J. -G., & Isaksson, E. (2001). Measuring snow and glacier ice properties from satellite. *Reviews of Geophysics*, *39*(1), 1–27.

Kouraev, A., Papa, F., Buharizin, P. I., Cazenave, A., Cretaux, J. F., Dozorsteva, J., & Rémy, F. (2003). Ice cover variability in the Caspian and the Aral Seas from active and passive satellite microwave data. *Polar Research*, *22*(1), 43–50.

Kuzmina, Z. V., & Treshkin, S. E. (1997). Soil salinization and dynamics of Tugai Vegetation in the Southeastern Caspian Sea Region and in the Aral Sea Coastal Region. *Eurasian Soil Science*, *30*(6), 642–649.

Legresy, B., & Remy, F. (1997). Altimetric observations of surface characteristics of the Antarctic ice sheet. *Journal of Glaciology*, *43*(144), 265–275.

Mercier, F., Cazenave, A., & Maheu, C. (2002). Interannual lake fluctuations (1993–1999) in Africa from Topex/Poseidon: Connections with ocean/atmosphere interactions over the Indian Ocean. *Global and Planetary Change*, *32*, 141–163.

Micklin, P. P. (1988). Desiccation of the Aral Sea. A water management disaster in the Soviet Union. *Science*, *241*, 1170–1175.

Moulin, S., Kergoat, L., Viovy, N., & Dedieu, G. (1997). Global scale assessment of vegetation phenology using NOAA/AVHRR satellite measurements. *Journal of Climate*, *10*(6), 1154–1170.

Njoku, E. G., & Li, L. (1999). Retrieval of land surface parameters using passive microwave measurements at 6–18 GHz. *IEEE Transactions on Geoscience and Remote Sensing*, *37*(1), 79–93.

Olson, J. S. (1992). World ecosystems (WE1.4). Global Ecosystem Database, V1.0: Disc A., Geophysical. Boulder, USA: Data Center.

Papa, F., Legresy, B., Mognard, N. M., Josberger, E. G., & Remy, F.

(2002). Estimating terrestrial snow depth with the Topex–Poseidon altimeter and radiometer. *IEEE Transactions on Geoscience and Remote Sensing*, *40*(10), 2162–2169.

Papa, F., Mognard, N. M., Josberger, E. G., & Remy, F. (2001). Snow signature with the ERS2 radar altimeter. *IGARSS'2001 Proceedings, Sydney, Australia, CD-Rom.*

Remy, F., Legresy, B., Bleuzen, S., Vincent, P., & Minster, J. F. (1996). Dual frequency Topex altimeter observations of Greenland. *Journal of Electromagnetic Waves and Applications*, *10*, 1507–1525.

Remy, F., Legresy, B., & Testut, T. (2001). Ice sheet and satellite altimetry. *Surveys in Geophysics*, *22*, 1–29.

Remy, F., Schaeffer, P., & Legresy, B. (1999). Ice flow physical processes derived from ERS-1 high resolution map of the Antarctica and the Greenland ice sheets. *Geophysical Journal International*, *139*, 645–649.

Rodriguez, E., & Martin, J. M. (1994). Assessment of the Topex–Poseidon altimeter performance using waveform retracking. *Journal of Geophysical Research*, *99*, 24977–24980.

Sherjal, I., & Fily, M. (1994). Temporal variations of microwave brightness temperatures over Antarctica. *Annals of Glaciology*, *20*, 19–25.

Sippel, S. J., Hamilton, S. K., Melack, J. M., & Novo, E. M. M. (1998). Passive microwave observations of inundation area and the area/stage relation in the Amazon river floodplains. *International Journal of Remote Sensing*, *19*, 3055–3074.

Ulaby, F. T., Moore, R. K., & Fung, A. K. (1982). Microwave remote sensing: Active and passive: Volume II. Radar remote sensing and surface scattering and emission. Norwood, USA: Addison-Wesley Publishing, Artech House.

Ulaby, F. T., Moore, R. K., & Fung, A. K. (1986). Microwave remote sensing: Active and passive: Volume III. From Theory to Applications. Norwood, USA: Addison-Wesley Publishing, Artech House.

Ye, H. C., Cho, H. R., & Gustafson, P. E. (1998). The changes in Russian winter snow cover accumulation during 1936–83 and its spatial pattern. *Journal of Climate*, *11*(5), 856–863.

Zieger, A. R., Hancock, D. W., Hayne, G. S., & Purdy, G. L. (1991). NASA radar altimeter for the Topex–Poseidon project. *IEEE Transactions on Geoscience and Remote Sensing*, *79*(6), 810–826.

Zwally, H. J., Bindschader, R. A., Brenner, A. C., Martin, T. V., & Thomas, R. H. (1983). Surface elevation contours of Greenland and Antarctica ice sheets. *Journal of Geophysical Research*, *88*, 1589–1596.